JOURNAL OF MATERIALS SCIENCE 31 (1996) 2091–2095

Influence of ferrite–martensite microstructural morphology on tensile properties of dual-phase steel

M. SARWAR
PAEC, Islamabad, Pakistan

R. PRIESTNER
Manchester Materials Science Centre, Manchester, UK

The influence of ferrite–martensite microstructural morphology, volume fraction of martensite, epitaxial ferrite on the tensile behaviour of dual-phase steels, was studied. It was observed that increasing the martensite content and its aspect ratio raised tensile strength and ductility. Epitaxial ferrite in rolled material strongly reduced the strength and improved the ductility, suggesting that substructure strengthening of material, as well as increased stress transfer to the hard phase, contribute to the strength of thermo-mechanically processed material. Mettallographic analysis of deformed samples revealed that void nucleation occurs predominantly along the ferrite–martensite interface. The void density in the necked region increased towards the fracture surface in all samples and was higher for samples which exhibited localized necking.

1. Introduction

The world oil crisis in the mid-1970s led to a demand for lighter, more efficient transport. The need to lower automobile vehicle weight and thereby improve fuel economy, has resulted in development of steel with increased strength/weight ratios. For example, Dinda *et al.* [1] have reported that decreasing an average car weight from 1750 kg to 1500 kg can improve the fuel consumption by up to $2\,km\,l^{-1}$. The high-strength microalloyed steels, however, suffer from the disadvantage that they show lower formability compared with conventional low-carbon steels which can necessitate a redesign of components. To overcome this disadvantage, dual-phase steels were developed as a new class of engineering materials, among the group of high-strength low-alloy steels.

Dual-phase steels comprise microstructures of 20%–25% hard phase martensite in relatively soft ductile and fine-grained ferrite matrix. Dual-phase steels have characteristic mechanical properties, which include low proof strength and high tensile strength, relative to conventional low-carbon formable steel. They also exhibit high work-hardening rates in the early stage of plastic deformation, and good ductility during forming relative to their strength in the formed condition. As a result, dual-phase steels play an important role in achieving a reduction in the weight of automobile components, such as car body panels, and accompanying benefits of fuel efficiency. Several [2–6] attempts have been made to describe the deformation behaviour and structure–properties relationships in dual-phase steels. Few have been concerned solely with the effect on mechanical properties of changes in the morphology of micro-constituents.

The objective of the present study was to investigate the influence of volume fraction of martensite, epitaxial ferrite microstructural morphology on tensile behaviour of dual-phase steel.

2. Experimental procedure

The chemical composition (wt %) of the steel used is given in Table I.

Each specimen was coded (e.g. 50BQ780) according to the treatment it was given. The left-hand number represents the amount of rolling deformation, the middle letters represents the cooling medium used (BQ = iced brine-quenched, HWQ = hot-water quenched and OQ = oil-quenched), and the right-hand number represents the intercritical annealing temperature.

2.1. Heat treatment for mechanical testing

In order to study tensile properties, blank 6 mm thick, 180 mm × 45 mm in area (for 0% reduction) and 12 mm thick and 130 mm × 45 mm in area) (for 50% reduction) were obtained from the original plates. These blanks were divided into four groups for intercritical heat treatment (ICHT) and thermo-mechanical processing (TMP) to obtain different volume fractions of martensite and microstructural morphology.

0022–2461

TABLE I The chemical composition (wt %) of steel used

Fe	C	Mn	Cr	Si	Mo
Balance	0.166	1.03	0.14	0.24	0.04

2.1.1. Group I
The blanks, 6 mm thick, were intercritically annealed at 780 °C for 20 min and quenched into iced brine or hot water (at 86 °C) to produce 55% and 30% martensite, respectively.

2.1.2. Group II
Blanks with 12 mm initial thickness were heat treated at 780 °C for 20 min, then rolled to a 50% reduction and quenched into iced brine or oil to produce the same amounts of martensite mentioned in Group I.

2.1.3. Group III
Blanks as in Group I were intercritically annealed at 740 °C for 20 min to produce 30% austenite and then quenched into iced brine.

2.1.4. Group IV
Blanks with the same initial thickness as in Group II were heat treated at 740 °C for 20 min and rolled to a 50% reduction and then quenched into iced brine.

2.2. Grain-size measurement
The average grain size was measured from photomicrographs using the mean linear intercept method. Three concentric circles, having diameters of 79.58, 53.05 and 26.53 mm, adding up to a total line length of 500 mm, were superimposed on photographic prints of the microstructure and the number of intercepts of the circle with ferrite grains were counted.

The main linear intercept in the ferrite, $\bar{d}_\alpha$, was calculated according to the following relationship [7]

$$\bar{d}_\alpha = \frac{V_\alpha L/M}{N_\alpha}$$

where L is the total test line length, V the volume fraction of ferrite, N the number of ferrite grains intercepted by the test line, and M the magnification of the print. A suitable magnification was used in order to obtain about 140 intercepts per field per phase. A total of about 550–650 intercepts were counted to get reasonable statistical accuracy.

2.3. Tensile testing
The tensile tests were performed using an Instron machine, model 1185, having 100 kN load capacity. The load was applied parallel to the rolling direction. All the tests were carried out at the crosshead speed of 0.5 mm min^{-1} in a normal atmosphere, at full-scale loads of either 10 or 15 kN. An Instron extensometer with gauge length of 12.5 mm was used until the specimens broke, and an autographic record of load versus per cent strain was also made. The proof stress was taken at 0.2% offset. Uniform elongation was designated as the elongation at which the load began to decrease, i.e. the onset of necking. Reduction in area and total elongation were also determined.

3. Results and discussion
3.1. Tensile properties
The tensile properties at room temperature of a specimen having different morphologies and volume fractions of martensite are listed in Table II. The true stress–true strain curves to the onset of necking were drawn. It was observed from the curves that, for all treatments, the microstructure gave rise to continuous yielding, which is one of the characteristics of dual-phase steels. In the ferrite–martensite steels, transformation of austenite to a strong second phase (i.e. martensite) introduces a high density of mobile dislocations in the surrounding polygonal ferrite matrix, which allows the steels to be deformed at low stresses with continuous yielding. The high density of mobile dislocation in a circular ferrite coupled with residual stresses from the martensite islands gives continuous yielding in a circular ferrite–martensite steel [7]. Fig. 1 shows the variation in 0.2% proof stress and tensile strength with the percentage of martensite after the various heat treatments and thermomechanical treatments. Both the 0.2% proof stress and UTS increased as martensite content increased, and both were higher in warmed rolled material that was brine-quenched. The presence of epitaxial ferrite in rolled material caused a marked decrease in strength.

Cai *et al.* [2] measured the tensile properties at room temperature of specimens with different martensite morphologies, but with approximately the same volume fraction of martensite, derived from various initial microstructures in 0.11% C, 1.6% Mn steel. Their results are listed in Table II for comparison. They showed that the highest strength was achieved in the specimen which received an intermediate quench, in which the martensite content after intercritical annealing was very fine and fibrous. The present data showed that the specimen 50BQ780 had the highest strength and was stronger than Cai *et al.*'s fibrous microstructure. This suggests that better stress transfer was obtained by fibring the martensite, both in Cai *et al.*'s experiments and reported here. For example, specimen 50BQ740 had higher strength than OBQ740 with the same volume fraction of martensite. Such fibring of martensite was achieved by rolling in the present work, and the fibring was aligned in the direction of tensile testing. In Cai *et al.*'s experiment, the fibring arose from austenite which formed along interlath boundaries present in the starting microstructure, and was random with respect to the tensile axis.

Speich and Miller [8] studied the tensile properties of a steel having the same carbon content as used in the present study. Some of their data are listed in

TABLE II Tensile properties of specimens with different volume fractions and morphology of martensite

Specimen code	Volume fraction of martensite	0.2% proof stress (MPa)	UTS (MPa)	Uniform elongation %	Total elongation (%)	True strain of fracture
		645	1012.33			
0BQ780	55.0	570	924.09	6.39	12.0	0.2693
		600	1014.76			
50BQ780	48.9	670	1068.63	5.87	8.9	0.3263
		360	703.78			
0HWQ780	27.0	357	645.57	5.75	10.0	0.4463
		365	694.16			
500Q780	32.0	305	690.85	8.09	17.3	0.4090
		270	667.34			
		450	834.65			
0BQ740	30.7	495	838.00	5.94	7.29	0.1544
		525	892.16			
50BQ740	29.4	516	871.28	5.34	8.0	0.1602
Banded A [2]	27	388	834	12	16	–
Homogeneous ferrite-pearlite B [2]	28	380	892	13	21	–
Lath martensite obtained by an intermediate quench C [2]	32	415	914	14	22	–
ICHT at 780 °C [8]	50.3	450	920	10.2	17.0	–
ICHT at 760 °C [8]	41.1	448	924	9.2	14.5	–
ICHT at 780 °C [8]	37.9	429	872	9.2	13.0	–

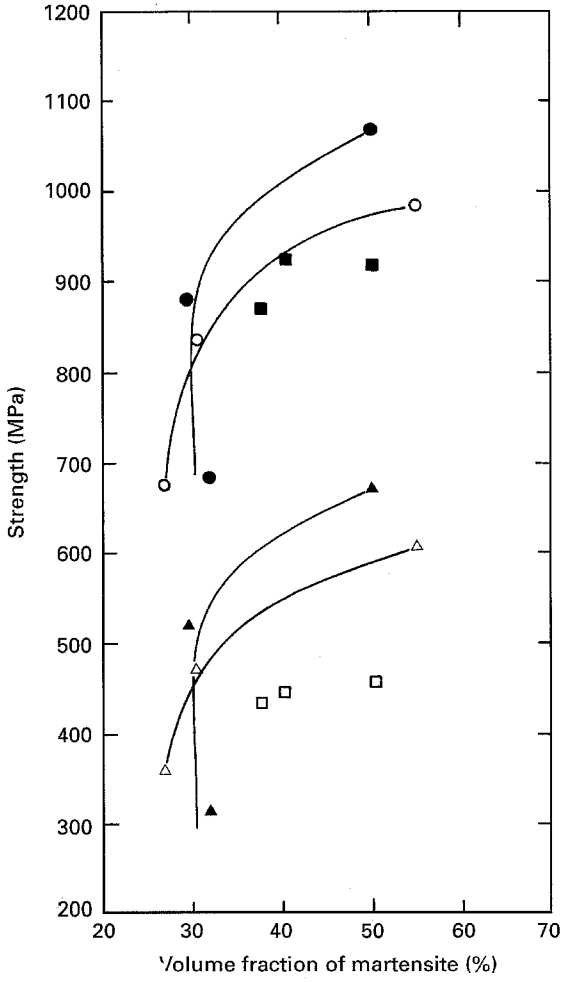

Figure 1 Variation in (●, ○, ■) tensile strength and (△, ▲, □) 0.2% proof stress versus the percentage of martensite; steel ICHT (○, △) not rolled and (●, ▲) warm rolled. (■, □) from [8].

Figure 2 Optical micrograph showing fibrous martensite and substructure in ferrite, specimen 50BQ780 × 1560.

Table II and are also plotted in Fig. 1 for comparison. Clearly, their proof strengths and tensile strengths were generally lower than observed here.

It is clear from metallographic observations that warm rolling caused a flattening and elongation of the austenite particles and a consequent fibring of the resultant martensite particles in the rolling direction. The increased aspect ratio of the martensite particles would be expected to improve stress transfer from the matrix to the particles during plastic deformation, and so increase strength. However, the effects of the rolling on the constitution of ferrite should also be considered. After rolling, ferrite grains are reduced in thickness, and this may give rise to an effective grain-refinement component of strengthening. It was also observed that a substructure was present in ferrite after rolling, as can be seen in Fig. 2. It appears, therefore, that effective ferrite grain refinement, the

substructure in ferrite, and the improved stress transfer to the fibred martensite, may all contribute to the improvement in strength brought about by rolling in the ($\alpha + \gamma$) phase field. This suggests that the addition of a rolling step during intercritical annealing is likely to be cheaper than addition of extra heat treatments to improve the tensile properties of dual-phase steel.

The specimen subjected to treatment 500Q780, containing epitaxial ferrite formed during and after rolling, had higher uniform and total elongations but lower proof and tensile strengths compared to all the specimens that were brine-quenched. The epitaxial ferrite would be expected to be relatively free of substructure, compared to old ferrite which had been deformed at the annealing temperature. This result also suggests that substructure strengthening of ferrite makes an important contribution to strength in warm-rolled dual-phase steel. Specimen OHWQ780 also contained epitaxial ferrite together with old ferrite that had not been rolled: its strength was similar to that of 500Q780, but its ductility was lower.

The fractographic study of the fracture surface of the specimens annealed at 780 °C and quenched in iced brine with or without rolling, exhibits large areas typical of cleavage fracture. This specimen had a fracture strain lower than specimen 50BQ780 which shows mixed modes of fracture. It can be noted that the specimens 0HWQ780 and 500Q780 containing approximately 20% epitaxial ferrite had high fracture strains compared to material that was almost free of epitaxial ferrite. It can also be seen that specimens 0BQ740 and 50BQ740 had approximately 50% less fracture strain compared to specimens 0BQ780 and 50BQ780. The fracture surfaces of specimens annealed at 740 °C and rolled to 0% and 48% reduction before quenching into iced brine exhibit large areas typical of cleavage fracture. The specimens annealed at 780 °C and rolled to 0% and 48% reduction before quenching into hot water or oil revealed that there is no trace of cleavage fracture. The fractured surfaces showed typical ductile fracture and microvoid coalescence as the dominant form of fracture. It is clear that the presence of epitaxial ferrite is associated with the ductile micromechanism of fracture in 0HWQ780 and 500Q780. Warm rolling had a weak influence in the same direction. However, the treatment which promoted higher true fracture strain by increasing the volume fraction of epitaxial ferrite did not give any improvement in tensile properties.

Examples of void formation in a necked region of fractured tensile specimens are shown in Figs 3–7. In general, void formation by decohesion at the interface of a hard inclusion in a ductile matrix must satisfy two criteria, an elastic-energy criterion and an interfacial-stress criterion [9]. The elastic-energy criterion is that the elastic energy which is stored in a plastically non-deformable inclusion and released during decohesion, must be greater than or equal to the increase in energy due to the newly formed free surface. This is why the particle/matrix interface must exceed the tensile strength of that interface before the stored elastic energy can be released to form the new surface.

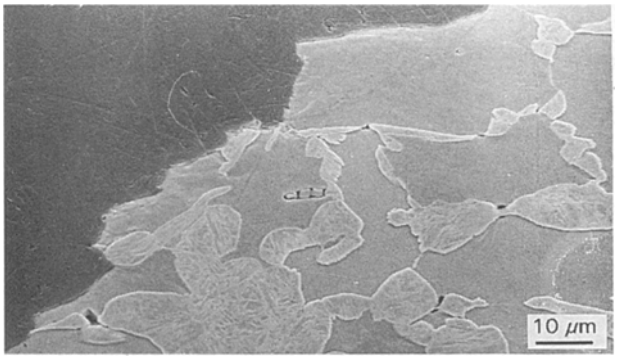

Figure 3 Scanning electron micrograph of a broken tensile specimen 0BQ780, indicating void formation.

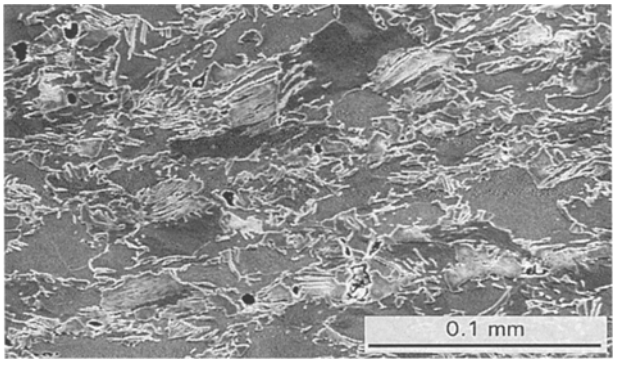

Figure 4 Scanning electron micrograph of a broken tensile specimen 0HWQ780, indicating void formation.

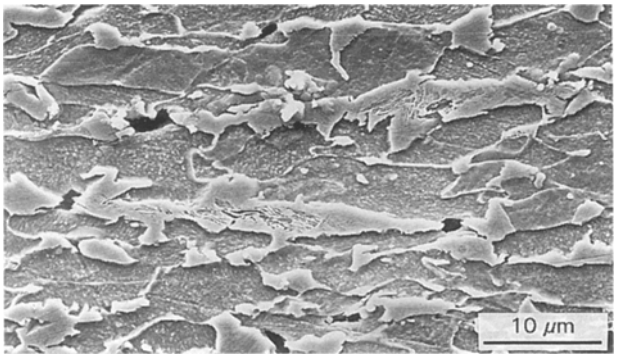

Figure 5 Scanning electron micrograph of a broken tensile specimen 500Q780, indicating void formation.

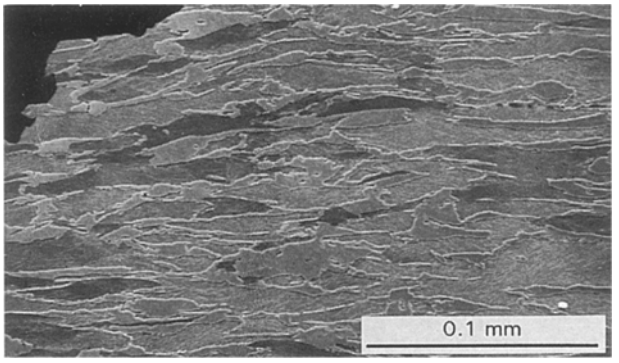

Figure 6 Scanning electron micrograph of a broken tensile specimen 50BQ740, showing no void formation.

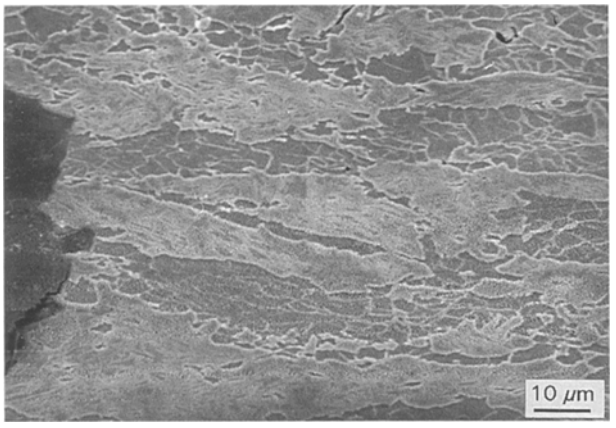

Figure 7 Scanning electron micrograph of a broken tensile specimen 50BQ780 showing no void formation.

The voids nucleated in the deformed samples occurred in three different, distinct locations associated with martensite particles. The first two, decohesion at ferrite–martensite interfaces and fracture of martensite, have been observed previously in dual-phase steels [11, 12]. The microstructure interface is indicated by arrows in the scanning electron micrographs shown in Fig. 13. In Fig. 4 the nucleation of voids by separation of fractured martensite particles is indicated by arrows on the micrographs.

The third mechanism, uniquely identified in this study, is illustrated in Fig. 5. In this mechanism, two separate martensite particles in line are separated at opposite ends of a void and the martensite particles protrude into the voids. Examples are indicated by arrows. The martensite particles are narrow and pointed, and they appear able to meet if the voids were to close. It is interpreted that these micrographs show void nucleation either from the separation of adjacent particles or as a consequence of localized deformation of the martensite.

It was observed from scanning electron micrographs that specimens 0HWQ780 and 500Q780 had higher densities of voids. These specimens had also higher true strains at fracture and approximately 20% epitaxial ferrite and 30% volume fraction of martensite. In contrast, specimens 0BQ740 and 50BQ740 showed remarkably low fracture strains and their microstructures were almost void free, as shown in Fig. 6. Specimens 50BQ740 and 50BQ780, which had elongated martensite particles, and were almost free of epitaxial ferrite, showed less tendency for void formation (Figs 6 and 7).

4. Conclusions

1. The warm rolling of the two-phase ($\alpha + \gamma$) mixture caused a useful increase in the strength of the rolling direction, provided that epitaxial ferrite was absent. This increase in strength caused flattening and elongation of austenite particles and consequent fibring of the resultant martensite particles in the rolling direction.

2. Strength also increased with increase of the volume of martensite and was reduced by the presence of epitaxial ferrite.

3. Ferrite grain refinement, substructure formation in ferrite and improved stress transfer to the fibred martensite, probably all contributed to the improvement in strength.

4. The addition of a rolling step during intercritical annealing is likely to be cheaper than the addition of extra heat treatments, for improving the tensile properties of dual-phase steel.

References

1. S. DINDA, J. A. DI CELLO and A. S. KASPER, "in Microalloying 75" (Union Carbide, Washington, 1975) p. 33.
2. XUE-LING CAI, J. FENG and W. S. OWEN, *Metall. Trans.* **16A** (1985) 1405.
3. C. A. N. LANZILLOTTO and F. B. PICKERING, *Met. Sci.* **16** (1982) 371.
4. X. G. HE, N. TERAO and A. BERGHEZANI, *ibid.* **18** (1984) 367.
5. R. G. DAVIES, *Metall. Trans.* **9A** (1978) 41.
6. G. TITHER and M. LAVITE, *J. Metals* **27** (1975) 15.
7. F. GEORGE VANDER VOURT, "Practical Applications Quantitative Metallographs", ASTM 839 (American Society for Testing and Materials, Philadelphia, PA, 1984) pp. 85–131.
8. G. R. SPEICH and R. L. MILLER, in "Structure and Properties of Dual-phase Steel", edited by R. A. Kot and J. W. Morris (AIME, 1979) pp. 145–80.
9. S. A. ARGON, J. IM. and R. SAFOGLU, *Metall. Trans.* **6A** (1975) 825.
10. J. R.FISHER and J. GURLAND, *Met. Sci.* **15** (1981) 193.
11. M. S. RASHID, in "Formable HSLA and dual-phase steels" edited by A. T. Davenport (TMS-AIME, New York, NY, 1979) pp. 1–24.
12. G. R. SPEICH and R. L. MILLER, in "Structure and Properties of dual-phase steels", edited by A. T. Davenport (TMS-AIME, New York. NY, 1979) pp. 58–86.
13. D. L. STEINBRUNNER, D. K. MATLOCK and G. KRAUSS, *Metall. Trans.* **19A** (1988) 759.

Received 15 February
and accepted 19 September 1995